J|A|C|S
ARTICLES
Published on Web 10/25/2005

Chirality- and Diameter-Dependent Reactivity of NO_2 on Carbon Nanotube Walls

Kwanyong Seo,[†] Kyung Ah Park,[‡] Changwook Kim,[†,§] Seungwu Han,[||] Bongsoo Kim,*[,†] and Young Hee Lee*[,‡]

Contribution from the Department of Chemistry, Korea Advanced Institute of Science and Technology (KAIST), Daejeon 305-701, Republic of Korea, Department of Physics, Center for Nanotubes and Nanostructured Composites, Sungkyunkwan University, Suwon 440-746, Republic of Korea, and Department of Physics and Division of Nano Science, Ewha Womans University, Seoul 120-750, Republic of Korea

Received April 19, 2005; E-mail: bongsoo@kaist.ac.kr; leeyoung@skku.edu

Abstract: We report the density-functional calculations of NO_2 adsorption on single-walled carbon nanotube walls. A single molecular adsorption was endothermic with an activation barrier, but a collective adsorption with several molecules became exothermic without an activation barrier. We find that NO_2 adsorption is strongly electronic structure- and strain-dependent. The NO_2 adsorption on metallic nanotubes was energetically more favorable than that on semiconducting nanotubes and furthermore the adsorption became less stable with increasing diameters of nanotubes. The adsorption barrier height shows similar dependence on the electronic structure and diameter to the adsorption energy. Our theoretical model can be a good guideline for the separation of nanotubes by electronic structures using various adsorbates.

Introduction

Despite superb applicabilities of carbon nanotubes (CNTs) to various types of devices, the device performance has not been fully optimized in many cases because of the coexistence of both semiconducting and metallic nanotubes in the sample. The electronic structure of single-walled carbon nanotubes (SWCNTs) is governed by the chiral index (n, m). When $n - m = 3k$, where k is an integer, the nanotubes become metallic and otherwise semiconducting.[1] Thus a significant fraction of the synthesized nanotubes is presumably metallic. This coexistence of CNTs with different electronic properties has been a hindrance for making effective electronic devices. It is therefore necessary to find out a method to prepare SWCNTs with a specific electronic structure either during synthesis or by some posttreatment, although the former has not been realized yet.

The sidewall functionalization of SWCNTs by dichlorocarbene, diazonium salts, fluorine gas, and atomic hydrogen transforms their electronic structure from metallic to semiconducting.[2−6] Atomic structures of the nanotube sidewall are modified sometimes by strong covalent bondings during the sidewall functionalization, which often leads to deformation of the local atomic structures of nanotubes and sometimes disintegrates the tubular structures.[7]

Another approach is to collect selectively either semiconducting or metallic SWCNTs. It has been proposed that dispersion of SWCNTs with octadecylamine (ODA) in tetrahydrofuran (THF) solvent reorganizes the ODA along the sidewall of SWCNTs, where the amine groups are physisorbed preferably on semiconducting SWCNTs.[8] Wrapping of SWCNTs by single-stranded DNAs has been suggested to be sequence-dependent, where the electrostatics of the DNA−SWCNT hybrid depends on tube diameters and electronic properties, enabling nanotube separation by an anion exchange chromatography.[9] A derivatized porphyrin can interact selectively with semiconducting SWCNTs in chloroform.[10] Despite such tremendous efforts, the yield of separation is not very high in most cases. Very recently, selective removal of metallic SWCNTs has been demonstrated by an attack of nitronium ions.[11] The selective attack to metallic nanotubes is also strongly diameter-dependent, although the

[†] KAIST.
[‡] Sungkyunkwan University.
[§] Current address: CAE team, Corporate R&D Center, Samsung SDI Co., Ltd. 428-5, Yongin 449-577, Korea.
[||] Ewha Womans University.

(1) Saito, R.; Fujita, M.; Dresselhaus, G.; Dresselhaus, M. S. *Appl. Phys. Lett.* **1992**, *60*, 2204.
(2) Kamaras, K.; Itkis, M. E.; Zhao, H.; Hu, B.; Haddon, R. C. *Science* **2003**, *301*, 1501.
(3) Strano, M. S.; Dyke, C. A.; Usrey, M. L.; Barone, P. W.; Allen, M. J.; Shan, H.; Kittrell, C.; Hauge, R. H.; Tour, J. M.; Smalley, R. E. *Science* **2003**, *301*, 1519.
(4) (a) Wang, Q.; Johnson, J. K. *J. Phys. Chem. B* **1999**, *103*, 4809. (b) Tada, K.; Furuya, S.; Watanabe, K. *Phys. Rev. B* **2001**, *63*, 155405. (c) Chan, S.-P.; Chen, G.; Gong, X. G.; Liu, Z.-F. *Phys. Rev. Lett.* **2001**, *87*, 205502.
(5) (a) Gölseren, O.; Yildirim, T.; Ciraci, S. *Phys. Rev. B* **2002**, *66*, 121401. (b) Kim, K. S.; Bae, D. J.; Kim, J. R.; Park, K. A.; Lim, S. C.; Kim, J. J.; Choi, W. B.; Park, C. Y.; Lee, Y. H. *Adv. Mater.* **2002**, *14*, 1818.
(6) (a) Mickelson, E. T.; Chiang, I. W.; Zimmerman, J. L.; Boul, P. J.; Lozano, J.; Liu, J.; Smalley, R. E.; Hauge, R. H.; Margrave. J. L. *J. Phys. Chem. B* **1999**, *103*, 4318. (b) An, K. H.; Heo, J. G.; Jeon, K. G.; Bae, D. J.; Jo, C.; Yang, C. W.; Park, C.-Y.; Lee, Y. H.; Chung, Y. S. *Appl. Phys. Lett.* **2002**, *80*, 4235.
(7) An, K. H.; Park, K. A.; Heo, J. G.; Lee, J. Y.; Jeon, K. K.; Lim, S. C.; Yang, C. W.; Lee, Y. S.; Lee, Y. H. *J. Am. Chem. Soc.* **2003**, *125*, 3057.
(8) Chattopadhyay, D.; Galeska, I.; Papadimitrakopoulos, F. *J. Am. Chem. Soc.* **2003**, *125*, 3370.
(9) Zheng, M.; et al. *Science* **2003**, *302*, 1545.
(10) Li, H.; Zhou, B.; Lin, Y.; Gu, L.; Wang, W.; Fernando, K. A. S.; Kumar, S.; Allard, L. F.; Sun, Y.-P. *J. Am. Chem. Soc.* **2004**, *126*, 1014.

10.1021/ja052556y CCC: $30.25

origin of such dependence on the electronic structures and diameters has not been clarified yet.

One of the main difficulties in increasing the yield of separation arises from the absence of theoretical models to explain the binding nature of adsorbates that could be strongly dependent on the electronic structure of nanotubes, although some theoretical calculations have been done with NO_2 molecules.[12,13] Our aim is to construct a theoretical model to explain the electronic structure-dependent adsorptions on SWCNTs by adsorbates. In this paper, we demonstrate a selective reactivity of NO_2 molecules on the sidewall of SWCNTs by calculating the adsorption energy and adsorption barrier height. The binding nature of NO_2, which relies strongly on the electronic structures and diameters of nanotubes, is explained in terms of the available electronic density of states at the Fermi level and the pyramidalization angle near the local C−O bond. The relevance of our theoretical model of the NO_2 molecule to the interpretation of nitronium ion treatment in experiment is further discussed.

Theoretical Approaches

We used a self-consistent, charge density functional based, tight-binding (SCC-DFTB) method to optimize adsorbed geometries of NO_2 molecules on the SWCNT sidewall. The charge transfer was taken into account through incorporation of a self-consistent scheme for Mulliken charges based on the second-order expansion of the Kohn−Sham energy in terms of charge density fluctuations.[14] We also used the density functional calculations within generalized gradient approximation (GGA) to check the validity of our tight binding calculations. We adopted Vanderbilt ultrasoft pseudopotential for ionic potentials.[15,16] The exchange-correlation energy in GGA was parametrized by Perdew and Wang's scheme.[17] The Kohn−Sham wave functions were expanded in plane waves with an energy cutoff of 35 Ry, which is necessary to maintain the accuracy of the total energy. We chose armchair and zigzag nanotubes for the calculations. The SCC-DFTB calculations were done with large supercells of 18 layers for armchair tubes and those of 20 layers for zigzag tubes along the tube axis with a periodic boundary condition. The convergence in the energy with different numbers of layers was tested.[18] We define an adsorption energy of molecules as $E_{ad.} = E_{tot.}(\text{adsorbate} + \text{CNT}) - E_{tot.}(\text{adsorbate}) - E_{tot.}(\text{CNT})$, where $E_{tot.}$ is the total energy of the system. Atoms were fully relaxed by the conjugate gradient method in SCC-DFTB and GGA calculations until the forces on each atom became less than 0.001 atomic units.

Results and Discussion

A. Adsorption Energetics. We first search for a stable adsorption geometry of a single NO_2 molecule. Figure 1 shows the side view of the several stable geometries of NO_2 adsorbed on the (9,0) zigzag nanotube optimized by the SCC-DFTB. The most stable configuration is shown in Figure 1a, where a single

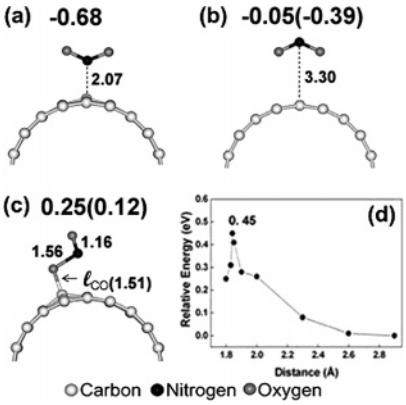

Figure 1. Optimized structures of the NO_2 molecule on the sidewall of the (9,0) nanotube: (a, b) physisorbed and (c) chemisorbed structures, and (d) absorption barrier for the chemisorbed structure (c). Dark, gray, and white balls indicate N, O, and C atoms, respectively. Adsorption energies in electronvolts are presented by the SCC-DFTB (GGA) calculations.

NO_2 molecule is adsorbed with the nitrogen atom placed toward the top carbon atom on the nanotube wall. This is called a *nitro* configuration, which is different from the nitration process where a nitrogen atom binds to an aromatic benzene ring.[19] The adsorption energy is −0.68 eV with a bond length of 2.07 Å, and this configuration has been predicted from calculations within local density approximation.[12,13,20] Although the binding energy is relatively large, the local geometries of the NO_2 molecule were not appreciably altered, and therefore we regard this as a physisorption. Figure 1b shows another stable geometry, called a *nitrito* configuration, where the nitrogen atom in NO_2 is placed 3.30 Å away from the nanotube sidewall. The adsorption energy obtained by the SCC-DFTB (GGA) calculation is −0.05 (−0.39) eV. No appreciable structural deformation on the NO_2 molecule is visible during this adsorption, simply a physisorption similar to Figure 1a.

An interesting local geometry is obtained, when one of the oxygen atoms in NO_2 approaches the tube wall, as shown in Figure 1c, similar to the previous report.[19,21] Even if we start from either the Figure 1a or Figure 1b configuration, Figure 1c will be the final configuration of oxygen adsorption via some rotation of the NO_2 molecule with possibly some additional barrier but not larger than that of Figure 1c during physisorption. In this case, the adsorption is endothermic with an adsorption energy of 0.25 (0.12) eV. Yet, this configuration is locally stable, as demonstrated from the detailed study of an adsorption barrier height in Figure 1d. In estimating the local barrier height, we fixed one oxygen atom located near the tube wall and relaxed the other atoms in the NO_2 molecule, including all the carbon atoms in the nanotube. This calculation was repeated by moving the NO_2 molecule close to the tube wall from a far distance. One can see from Figure 1d that the final adsorption energy is endothermic. Thus this geometry is kinetically limited. In this final geometry, the NO_2 molecule itself is severely distorted, i.e., the bond angle of O−N−O is reduced to 108° from 130° of an ideal NO_2 molecule, and bond lengths are changed to 1.56 and 1.16 Å from 1.21 Å, as shown in Figure 1c. This loses its

(11) An, K. H.; Park, J. S.; Yang, C.-M.; Jeong, S. Y.; Lim, S. C.; Kang, C.; Son, J.-H.; Jeong, M. S.; Lee, Y. H. *J. Am. Chem. Soc.* **2005**, *127*, 5196.
(12) Zhao, J.; Buldum, A.; Han, J.; Lu, J. P. *Nanotechnology* **2002**, *13*, 195.
(13) Peng, S.; Cho, K. *Nanotechnology* **2000**, *11*, 57.
(14) Elstner, M.; Shuhai, S.; Seifert, G. *Phys. Rev. B* **1998**, *58*, 7260.
(15) Baroni, S.; Dal Corso, A.; de Gironcoli, S.; Giannozzi, P. http://www.pwscf.org.
(16) Vanderbilt, D. *Phys. Rev. B* **1990**, *41*, 7892.
(17) Perdew, J. P.; Wang, Y. *Phys. Rev. B* **1992**, *45*, 13244.
(18) Special care was taken in the choice of the number of layers, particularly for an armchair tube because of the presence of π and π^* overlap at the Fermi level, which was located at 2/3 from the zone center. It was therefore crucial to choose an effective sampling point at the Fermi level to reveal the metallic characteristics. We chose 18 (multiple of six) layers for this purpose, and the total energy change from the choice of 24 layers was negligible. The total energy was saturated at these layers, as shown in the Supporting Information. It is interesting to see the dependence on the number of layers particularly on armchair nanotubes, which is related to the location of the Fermi level at 2/3 from the zone center.
(19) Ellison, M. D.; Crotty, M. J.; Koh, D.; Spray, R. L.; Tate, K. E. *J. Phys. Chem. B* **2004**, *108*, 7938.
(20) Chang, H.; Lee, J. D.; Lee, S. M.; Lee, Y. H. *Appl. Phys. Lett.* **2001**, *79*, 3863.
(21) Yim, W.-L.; Gong, X. G.; Liu, Z.-F. *J. Phys. Chem. B* **2003**, *107*, 9363.

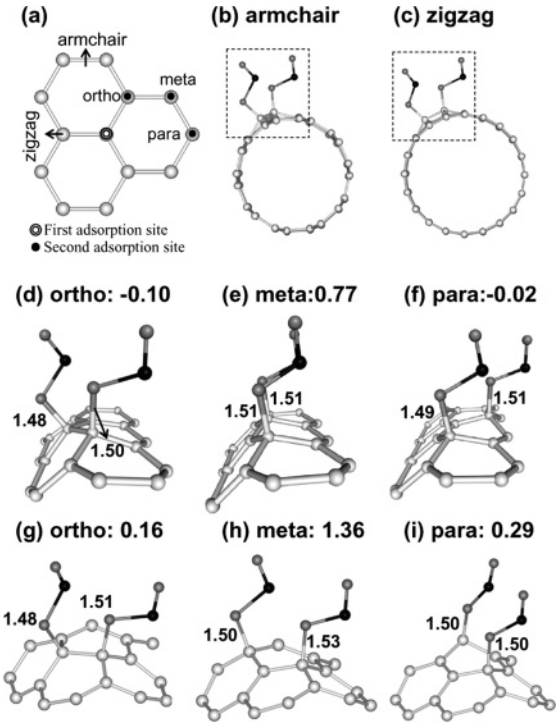

Figure 2. (a) Schematic view for adsorption sites of an additional NO_2 molecule on the nanotube wall and the top views of the adsorbed structure of (b) the (5,5) armchair nanotube and (c) the (10,0) zigzag nanotube. All other notations are similar to those in Figure 1. Panels d−f show the focused parts of the calculated adsorption sites for the adsorption of two NO_2 molecules on the sidewall of the (5,5) armchair nanotube, and g−i show those of the (10,0) zigzag nanotube. All other notations are as in Figure 1.

binding energy (1.89 eV), and furthermore the C−C back-bonds of the tube sidewall are also heavily strained with a distortion energy of 0.86 eV, where the distortion energy is defined as $E_d = E_{tot.}$(distorted SWCNT) − $E_{tot.}$(ideal SWCNT). However, the stabilization energy by the formation of a local C−O bond (l_{CO}) on chemisorption is huge (−2.51 eV), compensating most of the energy loss by the unfavorable distortion energy factors. This suggests that this locally stable geometry could be realized by an assistance of appropriate thermal energy. Since we are interested in the selective reactivity of nanotubes that may invoke a severe structural deformation that may lead to dissociation of the nanotube walls (oxidative etching),[22] we choose the chemisorbed geometry of Figure 1c for the rest of calculations to investigate the selective adsorption of the NO_2 molecule on particular nanotubes. Furthermore, this endothermic adsorption becomes exothermic with an additional NO_2 adsorption, as will be discussed in the following section. One may also consider several other types of adsorption such as a squeezed NO_2 molecule between two nanotubes. This is certainly a plausible geometry particularly in bundled nanotubes and will be investigated in the future.[19]

Figure 2 shows various chemisorption positions, when another NO_2 molecule is added to the configuration in Figure 1c. The energetics of associated adsorption is strongly site-dependent. The ortho position is the nearest adsorption site and the most favorable of all the sites listed here, allowing exothermic adsorption for both armchair and zigzag nanotubes. Significant energy loss due to heavy strain caused by the adsorption of the first NO_2 was now unnecessary with a strong C−O bond formed

(22) Herrera, J. E.; Resasco, D. E. *Chem. Phys. Lett.* **2003**, *376*, 302.

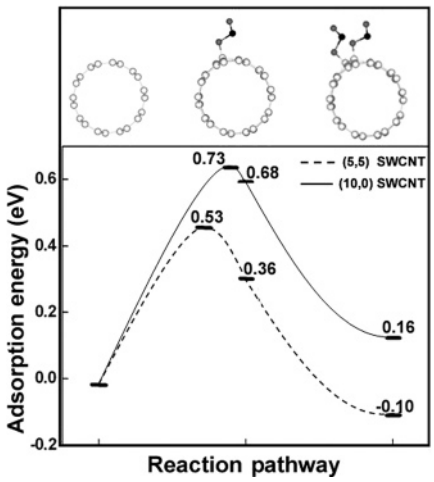

Figure 3. Adsorption energy of (5,5) SWCNT (dashed line) and (10,0) SWCNT (solid line) during NO_2 adsorption on the sidewall of SWCNT. All other notations are as in Figure 1.

by the second NO_2 adsorption in the ortho position. Some adjacent C−C back-bonds to NO_2 adsorption sites are severely weakened with bond lengths of 1.52, 1.59 Å. On the other hand, in para and meta adsorption sites, the distortion is simply spread at two nearly independent adsorption positions, resulting in relatively small energy gain. We emphasize that the adsorption becomes now exothermic in metallic (armchair) nanotubes, whereas it is still endothermic in semiconducting (zigzag) nanotubes. It has been well-known that oxygen treatment of nanotubes produces C−O bonds, which eventually leads to the dissociation of tube walls at high-temperature annealing.[23,24]

It is interesting to calculate an activation barrier height with the second NO_2 adsorption. The procedure to calculate activation barriers was similar to the single molecular adsorption. Figure 3 reveals a schematic reaction pathway with a series of NO_2 molecular adsorptions. When the first NO_2 molecule adsorbs on both nanotubes, activation barriers exist, making it possible to invoke kinetically limited adsorption. The activation barrier height was lower in metallic nanotube than in semiconducting nanotube, which will be discussed later. We would like to emphasize here that no adsorption barrier was observed in adsorption of the second NO_2 molecule, independent of the metallicity. Our calculations suggest that a collective exothermic adsorption in the adjacent sites is favored at high NO_2 concentration. In this case, the selective adsorption is determined solely by an adsorption energetics.

B. Diameter Dependence of Adsorption Energy and Adsorption Barrier Height. We next calculate the adsorption energy of armchair and zigzag nanotubes as a function of diameter, as shown in Figure 4a. This reveals two remarkable features. One is the dependence of adsorption energy on the electronic structures. Regardless of diameters, the adsorption to metallic (armchair) nanotubes is consistently stronger than that to semiconducting ones. In particular, all (3*n*,0) zigzag nanotubes, which are zero-band-gap semiconductors and simply

(23) (a) Zhu, X. Y.; Lee, S. M.; Lee, Y. H.; Frauenheim, T. *Phys. Rev. Lett.* **2000**, *85*, 2757. (b) Mazzoni, M. S. C.; Chacham, H.; Ordejon, P.; Sanchez-Portal, D.; Soler, J. M.; Artacho, E. *Phys. Rev. B* **1999**, *60*, 2208. (c) Mann, D. J.; Hase, W. L. *Phys. Chem. Chem. Phys.* **2001**, *3*, 4376. (c) Moon, C.-Y.; Kim, Y.-S.; Lee, E.-C.; Jin, Y.-G.; Chang, K. J. *Phys. Rev. B* **2002**, *65*, 155401.

(24) Seo, K.; Kim, C.; Choi, Y. S.; Park. K. A.; Lee, Y. H.; Kim, B. *J. Am. Chem. Soc.* **2003**, *125*, 13946.

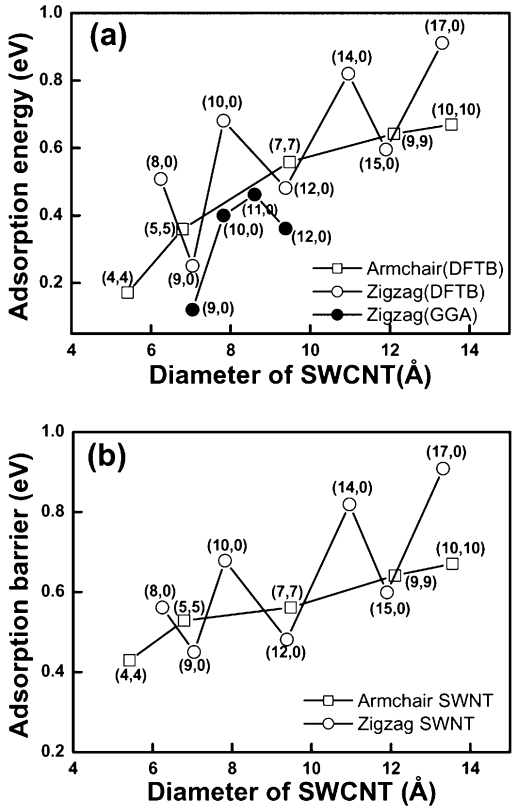

Figure 4. (a) NO_2 adsorption energy and (b) adsorption barrier height of armchair and zigzag nanotubes selected from Figure 1c as a function of nanotube diameter.

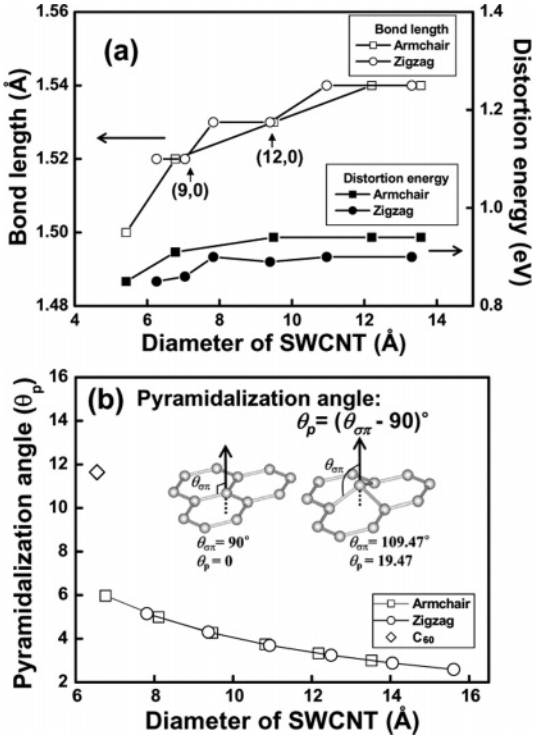

Figure 5. (a) Bond length of C(CNT)−O(NO_2), distortion energy of the nanotube wall, and (b) pyramidalization angle, as a function of nanotube diameter. The diamond shows that of fullerene.

regarded as metallic nanotubes,[25] show adsorption energies close to those of the armchair nanotubes. Another is the dependence of adsorption energy on diameters. The adsorption becomes weaker with increasing diameters in both metallic and semiconducting nanotubes. We have done more accurate calculations for zigzag nanotubes to check the validity of the SCC-DFTB. The GGA calculations give lower adsorption energies for zigzag nanotubes than the SCC-DFTB calculations, but show similar tendency that zero-gap zigzag nanotubes have consistently lower adsorption energies than nonzero-gap zigzag ones with the same diameter dependence. This confirms the validity of our calculations using the SCC-DFTB approach.

Figure 4b shows the adsorption barrier height as a function of diameter. The barrier heights of semiconducting nanotubes are consistently higher than those of metallic (armchair and (3*n*,0) zigzag) ones. The barrier height increases monotonically with increasing diameters in both armchair and zigzag nanotubes except the zero-gap (3*n*,0) zigzag nanotubes in which their barrier heights are similar to those of armchair nanotubes. Another interesting point to note is that the barrier exists only for small-diameter nanotubes of (4,4), (5,5), (8,0), and (9,0), independent of metallicity.[26] Others do not reveal the energy lowering after the transition point upon adsorption. Yet, the locally stable structure is maintained, which may be understood by a strong C−O bond between nanotube and NO_2 molecule despite the heavy distortion energy involved in other back-bonds of nanotube and NO_2 molecule. From this sense, the NO_2 molecule is an unusual adsorbate particularly at large diameters, compared to other types of adsorbates that show a typical transition state.[27] In case of large-diameter nanotubes with no transition state, the adsorption energy itself can be regarded as an adsorption barrier height, whereas in the case of small-diameter nanotubes, the adsorption barrier height is lowered by the presence of the transition state. This suggests that the selective adsorption is not only energetically controlled but also kinetically controlled at small-diameter nanotubes. Therefore, the selective adsorption could be enhanced in experiments by optimizing the reaction temperature in this case. However, at large-diameter nanotubes, the selectivity becomes less obvious due to the weak binding and the absence of transition state.

C. Diameter Dependence of Bond Length and Pyramidalization Angle. To understand the adsorption energetics of NO_2 as a function of diameter, we next calculate the bond length of l_{CO} and the distortion energy of the C−C network of nanotubes in Figure 5a. The distortion energy does not change appreciably with diameters (except the diameters less than 0.7 nm), revealing somewhat different behavior from the dependence of adsorption energy on diameters. On the other hand, l_{CO} increases gradually from 1.50 to 1.54 Å in armchair nanotubes, following the trend of changes in adsorption energy. In zigzag nanotubes, however, l_{CO} alternates, depending on the metallicity. It is of note that l_{CO} of metallic zigzag and armchair nanotubes almost coincides with each other at small diameters and furthermore the difference of l_{CO} between armchair and zigzag nanotubes at large diameters is nearly negligible. This strongly indicates that the abundance of the electronic density of states near the Fermi level determines the charge transfer, strengthening the binding of l_{CO}. This will be discussed later.

(25) Bulusheva, L. G.; Okotrub, A. V.; Romanov, D. A.; Tomanek, D. *J. Phys. Chem. A* **1998**, *102*, 975.
(26) See Supporting Information.
(27) Zhu, X. Y.; Lee, S. M.; Lee, Y. H.; Frauenheim, T. *Phys. Rev. Lett.* **2000**, *85*, 2757.

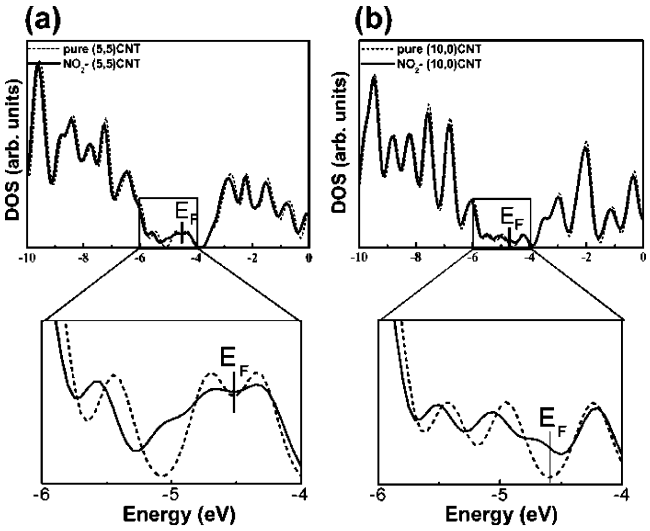

Figure 6. Electronic density of states (DOS) for (a) the (5,5) metallic nanotube and (b) the (10,0) semiconducting nanotube. The dashed and bold lines indicate the total DOS of the pure CNT and local DOS of the nanotube for the CNT + NO_2 system, respectively.

Our calculations suggest that l_{CO} dominantly governs the energetics of adsorption.

It is also interesting to note the change of pyramidalization angle (θ_p), as a measure of a degree of sp^3 hybridization, which is defined as $(\theta_{\sigma\pi} - 90)°$. Here the $\theta_{\sigma\pi}$ is the bond angle between σ and π bonds, as shown in Figure 5b.[28] This angle tells us the degree of sp^3 hybridization. Figure 5b shows a monotonic decrease in the pyramidalization angle with increasing diameters. In the case of C_{60}, θ_p is 11.6° and the strain energy is 0.35 eV/C, much larger than those of tubes with equivalent diameters of nanotubes.[29] We thus expect that the adsorption energy of NO_2 to C_{60} is much lower than those to nanotubes. Yet this value turns out to be 0.17 eV, not so much different from 0.25 eV of the (9,0) zigzag nanotube. This is ascribed to the semiconducting nature of C_{60} with an energy gap of 1.9 eV. This result suggests that the metallicity associated with strain of the nanotube is an important factor in determining the selective adsorption. At large diameters, the strain is reduced and the selectivity of adsorption between metallic and semiconducting nanotubes becomes obscured.[11]

D. Charge Transfer. Figure 6 shows the electronic density of states for (5,5) metallic and (10,0) semiconducting nanotubes. The charge density near the Fermi level is reduced in a metallic nanotube by 0.2 e due to charge transfer from the nanotube to NO_2, as shown in Figure 6a.[30] On the other hand, the (10,0) semiconducting nanotube has a finite band gap and thus no electronic density of states is available at the Fermi level. Instead of charge depletion at the Fermi level manifested in a metallic nanotube, the new gap states that originate from the oxygen atom in the NO_2 molecule bonded to the nanotube wall are developed near the Fermi level, as shown in Figure 6b, leading to a less favorable adsorption. This also agrees with the general belief that semiconductor has larger electron affinity than metal.

The interpretation of our calculations to experiments of nitronium ion (NO_2^+) treatment is rather subtle. We emphasize that NO_2 molecular adsorption on the CNT wall as described so far leads to a selective adsorption between metallic and semiconducting nanotubes. More importantly, this selectivity originates from the abundant presence of electron density near the Fermi level. In the case of NO_2^+ adsorption, however, this situation would not be much different from that of NO_2 molecular adsorption. The NO_2 molecule loses one electron from the lowest unoccupied molecular orbital and becomes NO_2^+. Consequently, NO_2^+ has stronger electron affinity than the NO_2 molecule. This will give stronger binding energy in metallic nanotubes than in semiconducting ones compared to NO_2 molecular adsorption. As a consequence we expect that the selectivity between metallic and semiconducting nanotubes would be more prominent in the case of nitronium ion.

Adsorbates can be classified into two categories: an acceptor-type and a donor-type. An adsorbate having atoms with larger electronegativity than carbon atoms (for instance oxygen atoms) is an acceptor-type.[21] It will induce charge transfer from a nanotube to an adsorbate, resulting in a higher binding energy due to partially ionic bonding character. The metallic nanotube has larger electron-charge density at the Fermi level than the semiconducting tube and therefore is expected to have a higher binding energy. For instance, NO_2 is an acceptor-type and prefers to be adsorbed on a metallic tube. On the other hand, the donor-type adsorbates would donate charges to nanotubes.[31] In this case, the semiconducting nanotube can accommodate charges more easily than the metallic nanotube because of higher electron affinity, giving rise to a higher binding energy. For instance, the amine group in ODA treatment and ammonia molecule are donor-type.[8,20] The ODA was selectively bound to semiconducting nanotubes, resulting in the separation of semiconducting nanotubes in the solution.[8] Although the selective adsorption is mostly governed by the available electron density at the Fermi level for NO_2 adsorption, the strain also tends to promote the adsorption and furthermore adsorption of NO_2 molecules induces heavy strains of C−C back-bonds in the tube wall. This may lead to the dissociation of the tube walls as observed in experiments.[11]

Summary

We found that the adsorption energy of NO_2 strongly relies on the electronic structure of nanotubes; i.e., NO_2 is adsorbed more strongly on metallic tubes than on semiconducting tubes. The available charge density at the Fermi level plays an important role for a favorable adsorption particularly with an acceptor-type adsorbate. Similar selectivity is also observed in the adsorption barrier height. We conclude that the adsorption of NO_2 molecule on carbon nanotube walls is both energetics- and kinetics-limited. The diameter dependence of adsorption energetics is explained by the pyramidalization angle and the bond length between the carbon and oxygen atoms. The energetics and kinetics in the chiral nanotubes are another interesting issue and will be investigated in the future.

Acknowledgment. This work is supported by the MOST through NT-IT Fusion Strategy of Advanced Technology,

(28) Niyogi, S.; Hamon, M. A.; Hu, H.; Zhao, B.; Bhowmik, P.; Sen, R.; Itkis, M. E.; Haddon, R. C. *Acc. Chem. Res.* **2002**, *35*, 1105.
(29) Oh, D.-H.; Lee, Y. H. *Phys. Rev. B* **1998**, *58*, 7407.
(30) The relative amount of charge transfer near the Fermi level was calculated by integrating the electronic density of states from −0.25 to 0.25 eV, where the Fermi level was taken to be zero. The change in the amount of charge transfer by a slight variance of the integration range was negligible.
(31) Kong, J.; Franklin, N. R.; Zhou, C.; Chapline, M. G.; Peng, S.; Cho, K.; Dai, H. *Science* **2000**, *287*, 622.

ABRL, and KOSEF through CNNC at SKKU and the 21st New Frontier Project, and BK21.

Supporting Information Available: Complete ref 9, Figure S1(the adsorption energy for a configuration of Figure 1a as a function of the number of layers along the *z*-axis in the supercell for (a) armchair (5,5) and (b) zigzag (10,0) nanotubes), and Figure S2 (the adsorption barrier for a configuration of Figure 1c: (a) zigzag (8,0), (b) zigzag (9,0), (c) armchair (4,4), and (d) armchair (5,5) nanotubes). This material is available free of charge via the Internet at http://pubs.acs.org.

JA052556Y